RESEARCH ARTICLE

Longitudinal Free-Water Changes in Dementia with Lewy Bodies

Shannon Y. Chiu, MD, MSc,[1,2*] Robin Chen, PhD,[3] Wei-en Wang, PhD,[3] Melissa J. Armstrong, MD, MSc,[1] Bradley F. Boeve, MD,[4] Rodolfo Savica, MD, PhD,[4] Vijay Ramanan, MD, PhD,[4] Julie A. Fields, PhD,[5] Neill Graff-Radford, MD,[6] Tanis J. Ferman, PhD,[7] Kejal Kantarci, MD,[8] David E. Vaillancourt, PhD,[3] and Alzheimer's Disease Neuroimaging Initiative

[1]*Department of Neurology, University of Florida, Gainesville, Florida, USA*
[2]*Department of Neurology, Mayo Clinic, Scottsdale, Arizona, USA*
[3]*Laboratory for Rehabilitation Neuroscience, University of Florida, Gainesville, Florida, USA*
[4]*Department of Neurology, Mayo Clinic, Rochester, Minnesota, USA*
[5]*Department of Psychiatry and Psychology, Mayo Clinic, Rochester, Minnesota, USA*
[6]*Department of Neurology, Mayo Clinic, Jacksonville, Florida, USA*
[7]*Department of Psychiatry and Psychology, Mayo Clinic, Jacksonville, Florida, USA*
[8]*Department of Neuroradiology, Mayo Clinic, Rochester, Minnesota, USA*

ABSTRACT: Background: Diffusion-weighted magnetic resonance imaging (dMRI) examines tissue microstructure integrity in vivo. Prior dementia with Lewy bodies (DLB) diffusion tensor imaging studies yielded mixed results.

Objective: We employed free-water (FW) imaging to assess DLB progression and correlate with clinical decline in DLB.
Methods: Baseline and follow-up MRIs were obtained at 12 and/or 24 months for 27 individuals with DLB or mild

***Correspondence to:** Dr. Shannon Y. Chiu, Department of Neurology, Mayo Clinic Arizona, 13400 East Shea Blvd, Scottsdale, AZ 85259, USA; E-mail: chiu.shannon@mayo.edu

Data used in the preparation of this article were obtained from the Alzheimer's Disease Neuroimaging Initiative (ADNI) database (adni.loni.usc.edu). As such, the investigators within the ADNI contributed to the design and implementation of ADNI and/or provided data but did not participate in the analysis or writing of this report. A complete listing of ADNI investigators can be found at http://adni.loni.usc.edu/wp-content/uploads/how_to_apply/ADNI_Acknowledgement_List.pdf.

Relevant conflicts of interest/financial disclosures: S.Y.C. receives research support from the National Institutes of Health (NIH) (K23 AG073525-01A1), Harry T. Mangurian Jr. Foundation, and Smallwood Foundation. R.C. has no relevant disclosures. W.W. has no relevant disclosures. M.J.A. receives research support from NIH (R01AG068128, P30AG047266, R01NS121099, R44AG062072), and as the local Principal Investigator (PI) of a Lewy Body Dementia Association Research Center of Excellence. She serves on the Data Safety Monitoring Boards (DSMBs) for the Alzheimer's Therapeutic Research Institute/Alzheimer's Clinical Trial Consortium and the Alzheimer's Disease Cooperative Study. She has provided educational content for Medscape, Vindico CME, and Prime Inc. B.F.B. receives honorarium for scientific advisory board (SAB) activities for the Tau Consortium, institutional research grant support from the Lewy Body Dementia Association, American Brain Foundation, Alector, Biogen, Transposon, and GE Healthcare. R.S. receives support from the National Institute on Aging, the National Institute of Neurological Disorders and Stroke, the Parkinson's Disease Foundation, and Acadia Pharmaceuticals. V.R. receives research support from NIH. J.A.F. receives research support from NIH. N.G.-R. receives research support as the local PI of a Lewy Body Dementia Association Research Center of Excellence and from NIH. T.J.F. receives research support from NIH, the Mayo Clinic Dorothy and Harry T. Mangurian Jr. Lewy Body Dementia Program, and Ted Turner and Family LBD Functional Genomics Program. K.K. receives research support from NIH, Avid Radiopharmaceuticals, Eli Lilly and consults for Biogen. D.E.V. receives research support from NIH and is Co-Founder of Automated Imaging Diagnostics.

Funding agencies: Supported by National Institutes of Health (NIH) grants K23 AG073525-01A1, U01 NS100620, U19 AG71754, P30 AG62677, R01 AG068128, P30 AG047266, R01 NS058487, R01 NS121099, RF1NS121099, R44 AG062072; the Robert H. and Clarice Smith and Abigail Van Buren Alzheimer s Disease Research Program of the Mayo Foundation; the Lewy Body Dementia Association; the Mayo Clinic Dorothy and Harry T. Mangurian Jr. Lewy Body Dementia Program; the Little Family Foundation; and Ted Turner and Family LBD Functional Genomics Program. Data collection and sharing for this project was also funded by the Alzheimer's Disease Neuroimaging Initiative (ADNI) (NIH grant U01 AG024904) and Department of Defense (DOD) ADNI (DOD award number W81XWH-12-2-0012). ADNI is funded by the National Institute on Aging, the National Institute of Biomedical Imaging and Bioengineering, and through generous contributions from the following: AbbVie, Alzheimer's Association; Alzheimer's Drug Discovery Foundation; Araclon Biotech; BioClinica, Inc.; Biogen; Bristol-Myers Squibb Company; CereSpir, Inc.; Cogstate; Eisai Inc.; Elan Pharmaceuticals, Inc.; Eli Lilly and Company; EuroImmun; F. Hoffmann-La Roche Ltd and its affiliated company Genentech, Inc.; Fujirebio; GE Healthcare; IXICO Ltd.; Janssen Alzheimer Immunotherapy Research & Development, LLC.; Johnson & Johnson Pharmaceutical Research & Development LLC.; Lumosity; Lundbeck; Merck & Co., Inc.; Meso Scale Diagnostics, LLC.; NeuroRx Research; Neurotrack Technologies; Novartis Pharmaceuticals Corporation; Pfizer Inc.; Piramal Imaging; Servier; Takeda Pharmaceutical Company; and Transition Therapeutics. The Canadian Institutes of Health Research is providing funds to support ADNI clinical sites in Canada. Private sector contributions are facilitated by the Foundation for the National Institutes of Health (www.fnih.org). The grantee organization is the Northern California Institute for Research and Education, and the study is coordinated by the Alzheimer's Therapeutic Research Institute at the University of Southern California. ADNI data are disseminated by the Laboratory of NeuroImaging at the University of Southern California.

Received: 16 October 2023; **Revised:** 6 January 2024; **Accepted:** 16 February 2024

Published online in Wiley Online Library (wileyonlinelibrary.com). DOI: 10.1002/mds.29763

cognitive impairment with Lewy bodies (MCI-LB). FW was analyzed using the Mayo Clinic Adult Lifespan Template. Primary outcomes were FW differences between baseline and 12 or 24 months. To compare FW change longitudinally, we included 20 cognitively unimpaired individuals from the Alzheimer's Disease Neuroimaging Initiative.
Results: We followed 23 participants to 12 months and 16 participants to 24 months. Both groups had worsening in Montreal Cognitive Assessment (MoCA) and Movement Disorder Society-Unified Parkinson's Disease Rating Scale (MDS-UPDRS) scores. We found significant FW increases at both time points compared to baseline in the insula, amygdala, posterior cingulum, parahippocampal, entorhinal, supramarginal, fusiform, retrosplenial, and Rolandic operculum regions. At 24 months, we found more widespread microstructural changes in regions implicated in visuospatial processing, motor, and cholinergic functions. Between-group analyses (DLB vs. controls) confirmed significant FW changes over 24 months in most of these regions. FW changes were associated with longitudinal worsening of MDS-UPDRS and MoCA scores.
Conclusions: FW increased in gray and white matter regions in DLB, likely due to neurodegenerative pathology associated with disease progression. FW change was associated with clinical decline. The findings support dMRI as a promising tool to track disease progression in DLB. © 2024 International Parkinson and Movement Disorder Society.

Key Words: dementia with Lewy bodies; diffusion-weighted imaging; Lewy body disease; magnetic resonance imaging

Dementia with Lewy bodies (DLB) is a common cause of late-onset neurodegenerative dementia, accounting for 15–20% of autopsy-confirmed dementias.[1,2] Together with Parkinson disease (PD), DLB is a Lewy body disease caused by abnormal aggregation of α-synuclein in Lewy bodies and neurites. Individuals with DLB present with dementia, rapid eye movement sleep behavior disorder (RBD), cognitive fluctuations, visual hallucinations, and/or parkinsonism.[2] Mild cognitive impairment (MCI) can precede the dementia of DLB, termed MCI-LB.[3] Executive MCI and hippocampal preservation on MRI are strong predictors of progression from MCI-LB to probable DLB (vs. Alzheimer's disease [AD]).[4,5]

Diffusion magnetic resonance imaging (dMRI) is a promising, non-invasive, in vivo method to evaluate tissue integrity changes in neurodegenerative disorders, especially when volumetric changes are not yet detectable in early disease stages.[6-9] dMRI assesses tissue integrity based on water diffusion changes within the brain, which can be influenced by pathology affecting axons, myelin, cerebrospinal fluid (CSF), neuronal soma, and dendrites. Water diffusion in the brain can be isotropic (ie, equal diffusion in all directions as in CSF and gray matter) or anisotropic (ie, unidirectional diffusion as in white matter).[10] Most dMRI studies in DLB used a diffusion tensor imaging (DTI) approach to evaluate white matter microstructure. Fractional anisotropy (FA, quantifying anisotropic diffusion) and mean diffusivity (MD, quantifying total diffusivity) are common diffusion measures in these studies.

Prior DTI studies in DLB have variable results.[11] Some found widespread disruptions involving frontal, temporal, insular, cingulate, parietal, occipital, callosal, and visual association areas.[12,13] Others reported more localized disruptions in parietal and occipital regions with sparing of frontal regions.[14,15] Several studies reported consistent disruptions of the inferior longitudinal, uncinate, superior longitudinal, and inferior fronto-occipital fasciculi implicated in disruptions of visual association pathways in DLB.[16-20]

In the only prior longitudinal DLB dMRI study, patients with DLB, AD, and healthy controls were followed for 1 year.[21] The study found no longitudinal change in MD or FA in patients with DLB compared to controls.

The variable results in DLB from prior dMRI studies could relate to known limitations of the conventional DTI approach and different analyses used to assess structural connectivity. DTI does not consider non-Gaussian diffusion properties in certain brain tissue compartments (eg, cell membrane and myelin sheath) or volumetric effects from extracellular free-water (FW) (eg, CSF).[22] DTI shortcomings include its inability to evaluate microstructural changes in gray matter, leading to inaccurate diffusion measures at the gray–white matter boundaries due to presence of extracellular FW.[6,22] Other considerations are the variable use of manual region of interest (ROI) selections,[12] tract-specific method,[17] voxel-based approaches,[13] probabilistic tractography,[23] or tract-based spatial statistics.[14]

Here, we applied a robust and established dMRI analysis technique with FW mapping, a two-compartment model that explicitly separates extracellular diffusing water from brain tissue. We previously showed FW to be a viable marker of tracking disease progression in parkinsonian disorders and AD.[9,24,25] For example, studies showed elevated FW within the posterior substantia nigra (SN) in PD, compared to more widespread networks in patients with atypical parkinsonian syndromes.[8,25] FW increases longitudinally in the posterior SN in PD, but not controls, further supporting FW as a promising progression marker.[24] FW increases are linked to neuroinflammation and myelin changes in neurodegenerative disorders.[26] We applied a FW dMRI technique to better characterize diffusion changes in DLB and hypothesized that FW would be elevated in affected regions in DLB.

We investigated longitudinal FW changes in individuals with DLB and cognitively healthy adults, and evaluated cognitive and motor markers of clinical progression in relation to dMRI.

Methods

Participants

Participants met criteria for probable MCI-LB[3] or DLB[2] and were enrolled in the single-center Mayo Clinic Longitudinal Imaging Biomarkers of DLB program (Rochester, MN, USA; enrolled 6/2018–3/2022). Participants with DLB/MCI-LB were also recruited as part of the Mayo Clinic Alzheimer Disease Research Center. Clinical diagnosis was determined by consensus conference. Participants meeting criteria for MCI-LB[3] had MCI and at least one core clinical feature (ie, parkinsonism, fluctuations, visual hallucinations, RBD).[3] Participants with DLB met probable DLB criteria from the Fourth Consortium Criteria.[2] Participants were followed with at least two clinical evaluations with MRI at baseline and 12 and/or 24 months.

A cohort of cognitively unimpaired individuals was included from the Alzheimer's Disease Neuroimaging Initiative (ADNI) database (http://adniloni.usc.edu) for comparative analyses. ADNI was launched in 2003 as a public–private partnership. ADNI's primary goal is testing whether serial MRI, positron emission tomography (PET), other biological markers, clinical, and neuropsychological assessment can be combined to measure MCI progression and early AD. Controls from ADNI were matched to DLB/MCI-LB participants based on age, sex, and common cardiovascular comorbidities. Controls were included only if they had baseline MRI with follow-up at ≥24 months (range 2–3 years).

Clinical Evaluation

Participants with DLB/MCI-LB underwent comprehensive evaluations.[27] Clinical features of DLB were assessed via history and validated scales. Cognitive fluctuations were assessed using the four-item Mayo Fluctuations Scale.[28] Visual hallucinations were fully formed occurrences, and not restricted to a single episode or related to other medical issue/treatment. History of probable RBD was based on the International Classification of Sleep Disorders-II diagnostic criteria.[29] Parkinsonism was based on neurologic examination, and the Movement Disorder Society-Unified Parkinson's Disease Rating Scale (MDS-UPDRS).[30] The Montreal Cognitive Assessment (MoCA) total score assessed global cognition.

Standard Protocol Approvals, Registrations, and Patient Consents

All participants with DLB/MCI-LB and/or their proxies provided informed consent. The Mayo Clinic Institutional Review Board (IRB) approved the study procedures (IRB ID# 17–011339). Data for cognitively unimpaired individuals from ADNI are publicly available as part of a multisite longitudinal biomarker research program, approved by IRBs at all participating locations.

dMRI Acquisition

All participants with DLB/MCI-LB underwent 3 T MRI with a 64-channel phased array head coil (Siemens). Diffusion scans were acquired with the following parameters: TR = 3400–4300 ms, TE = 71–99 ms, multi-shell acquisition (b-value = 0, 500, 1000, 2000 mm^2/s), angular resolution of 108 directions, in-plane voxel size of 2–2.26 mm in the x-dimension and 22.26 mm in the y-dimension, and slice thickness = 2 mm. We extracted the imaging data with b-value = 0, 1000 for FW imaging analyses using the algorithm from prior work[31]; two shells were used to harmonize analyses for DLB and controls (as non-multi-shell images were obtained prior to ADNI3). MRIs for controls were obtained from the ADNI databases Phase 2 and 3 (adni.loni.usc.edu). Axial diffusion weighted images (with or without multiband) were acquired on 3 T scanners (Siemens = 18, GE = 4, Philip = 18) with a whole-brain echo planar sequence with the following parameters: gradient directions = 31–61, b-value = 1000, TR = 3400–16,700 ms, TE = 55–105 ms, in-plane voxel size of 0.9–2.7 mm in x-dimension and 0.9–2.7 mm in y-dimension, and slice thickness = 2 or 2.7 mm (no gap).

dMRI Data Analysis

The primary outcome was FW across 122 ROIs. dMRIs were processed with image processing tools from the FMRIB Software Library (FSL[32,33]), Advance Normalization Tools (ANTs),[34] and custom UNIX shell scripts. The dMRI processing pipeline was completely automated, and results were consistent with prior work.[8,9] The normalization and image processing pipeline used was previously validated in the Appendix from the Archer et al. study.[8] Scans were corrected for distortions due to eddy currents and head motion with affine transformations.[33] The gradient directions were subsequently rotated to reflect these corrections, and non-brain tissue regions were removed from the scans.[32] DTIFIT was used to calculate b0 and FA images. Intermediate outputs were visually inspected to ensure absence of structural abnormalities (eg, stroke, tumor) or any anomalies with generated FW maps, such as poor normalization.[8] FW maps were calculated using custom written MATLAB R2020b

(The Mathworks) codes.[24,31] This code implemented a minimization procedure that fits a bi-tensor model, quantifying the fractional volume of FW in each voxel (ie, FW maps), as previously described.[24] The bi-tensor model predicts the signal attenuation in the presence of FW contamination. It is the sum of attenuations from two compartments: one modeling FW, and a second tissue compartment modeling water molecules in the vicinity of tissue membranes.[24] For the normalization pipeline, we used rigid alignment and Symmetric Normalization (SyN) in ANTs software using a FA map as the template image, which was created by averaging 100 Human Connectome Project (HCP) (http://www.humanconnectomeproject.org) subjects in Montreal Neurological Institute (MNI) space. The FA map image was linearly registered to a mean HCP FA template, followed by a nonlinear transformation using SyN. The implementation of this technique is consistent with prior work[7-9,24] and is validated in the Appendix from the Archer et al. study.[8]

ROIs

ROIs included gray and white matter, and were created based on the atlas from the Mayo Clinic Adult Lifespan Template (MCALT; https://www.nitrc.org/projects/mcalt/).[35] The MCALT was specifically designed for analysis of MRIs of adults aged 30+ years. Recent studies on neurodegenerative disorders, including DLB, have used the MCALT.[36,37] Diffusion measures were calculated separately for left and right hemispheric ROIs in the MCALT template.

Statistical Methods

Longitudinal change for demographic and clinical variables was assessed with Pearson's χ^2, independent, or paired *t*-tests as appropriate. Mean change from baseline to follow-up in FW maps for participants with DLB/MCI-LB was calculated for each ROI using paired *t*-tests. Significant ROIs were corrected for multiple comparisons using the false discovery rate (FDR) method[38] ($p_{fdr} < 0.05$). To assess FW change longitudinally in cognitively unimpaired individuals, we applied paired *t*-tests and within-subject ANCOVA with repeated measures controlling for imaging site. We then conducted a one-way ANCOVA to identify ROIs with significant differences between DLB/MCI-LB and controls based on FW change over 2 years, controlling for age, baseline FW, and imaging site. We selected the one-way ANCOVA model as it accounts for the study design with multisite controls and relies on the computed FW change to focus on longitudinal change. Secondary analyses with linear regressions were performed to determine the association of longitudinal change in diffusion measures and baseline FW, with clinical disease progression based on change in MoCA and MDS-UPDRS scores. Only the regions with significant changes in diffusion measures for FW (at 12 or 24 months follow-up in DLB/MCI-LB) were entered in forward linear regression models. Statistical analyses were performed in IBM SPSS version 28.0.

Results

Demographics and Clinical Assessment

Twenty-three individuals (n = 3 MCI-LB, n = 20 DLB; mean age 69.3 ± 9.5 years; 95% male) completed evaluations at baseline and 12 months. Sixteen individuals (n = 2 MCI-LB, n = 14 DLB; mean age 67.5 ± 9.3 years; 100% male) completed evaluations at baseline and 24 months (Table 1). Twelve participants had follow-ups at 12 and 24 months. Twenty cognitive unimpaired individuals (mean age 70.2 ± 2.1 years; 100% male) completed evaluations at baseline and ≥ 24 months (Table 1).

MoCA and MDS-UPDRS (Total, Part III) scores significantly declined from baseline to 12 months and 24 months in the DLB/MCI-LB cohort (all $P < 0.05$; Table 2). Hoehn and Yahr stage did not differ for either interval. MoCA scores did not change significantly in controls (Table 2).

FW Imaging Changes at 12 Months in DLB/MCI-LB

FW increased from baseline to 12 months for participants with DLB/MCI-LB in the left pallidum, left amygdala, left entorhinal cortex, bilateral insula, bilateral posterior cingula, left parahippocampus, bilateral Rolandic operculum, left fusiform, right retrosplenial cortex, right lingual gyrus, and right supramarginal gyrus (all $p_{fdr} < 0.05$) (Table 3).

Greater Network of FW Imaging Changes at 24 Months in DLB/MCI-LB

Apart from the right lingual gyrus and left pallidum, the same ROIs that showed FW increases in DLB/MCI-LB from baseline to 12 months were also identified at 24 months. Specifically, the left amygdala, bilateral posterior cingula, left entorhinal cortex, left parahippocampus, bilateral insula, left fusiform, right retrosplenial cortex, bilateral Rolandic operculum, and right supramarginal gyrus were associated with significant FW increases from baseline to 24 months ($p_{fdr} < 0.05$) (Table 3, Fig. 1). Additional ROIs had significant FW increases at 24 months only: anterior and posterior SN, pallidum, putamen, mid cingulum, hippocampus, inferior frontal, superior temporal, and thalamus regions (Table 3, Fig. 2).

In cognitively unimpaired individuals, there were no significant changes surviving FDR correction in any ROI (baseline to ≥24 months) (Table S1). There was no significant effect of imaging site. To compare

TABLE 1 *Patient characteristics*[a]

Characteristic	DLB with 12 months follow-up (n = 23)	DLB with 24 months follow-up (n = 16)	Cognitively unimpaired with ≥24 months follow-up (n = 20)
Age at baseline visit, y (SD)	69.3 (9.5)	67.5 (9.3)	70.2 (2.1)
Male, n (%)	22 (96)	16 (100)	20 (100%)
Education, y (SD)	15.6 (4.0)	15.5 (3.4)	16.6 (2.0)
Cholinesterase inhibitor, n (%)	14 (61)	8 (50)	N/A
Levodopa use at baseline and/or follow-up, n (%)	10 (43.4)	8 (50)	N/A
Primary clinical diagnosis, n (%)			
MCI-LB[b,c]	3 (13)	2 (13)	N/A
DLB	20 (87)	14 (87)	N/A
Medical comorbidities, n (%)[d]			
History of smoking	6 (26.1)	2 (12.5)	0
Hypertension	5 (21.7)	4 (25)	8 (40)
Hyperlipidemia	9 (39.1)	4 (25)	4 (20)
History of stroke	1 (4.3)	0	0

Abbreviations: DLB, dementia with Lewy bodies; y, years; SD, standard deviation; N/A, not applicable; MCI-LB, mild cognitive impairment with Lewy bodies.
[a]Twelve patients had follow-up at both 12 months and 24 months. Most participants were non-Hispanic (91% in 12-month cohort; 100% in 24-month cohort), and White (100% in 12-month cohort; 94% in 24-month cohort). All cognitively unimpaired individuals were non-Hispanic and White.
[b]Additional demographic/clinical information for subjects with MCI-LB with 12 months follow-up (n = 3): mean age 62 ± 15 years, 100% male, mean education 15.3 ± 3.1 years, 100% taking cholinesterase inhibitor, 0% taking levodopa, mean baseline total Montreal Cognitive Assessment (MoCA) score 20 ± 7, mean baseline total Movement Disorder Society-Unified Parkinson's Disease Rating Scale (MDS-UPDRS) score 40 ± 13.
[c]Additional demographic/clinical information for subjects with MCI-LB with 24 months follow-up (n = 2): mean age 80 ± 7 years, 100% male, mean education 15.0 ± 4.2 years, 50% taking cholinesterase inhibitor, 50% taking levodopa, mean baseline total MoCA score 17 ± 4, mean baseline total MDS-UPDRS score 36 (missing baseline MDS-UPDRS score for 1 subject).
[d]Cognitively unimpaired individuals from the Alzheimer's Disease Neuroimaging Initiative (ADNI) were matched to DLB/MCI-LB participants (24 months) based on age, sex, and common cardiovascular comorbidities (eg, history of smoking, hypertension, hyperlipidemia, and prior stroke; all $P > 0.05$).

TABLE 2 *Clinical changes from baseline to 12 or 24 months*

Clinical scale	Baseline	DLB/MCI-LB at 12 months (n = 23)	*P*-value	Baseline	DLB/MCI-LB at 24 months (n = 16)	*P*-value	Baseline	Cognitively unimpaired with ≥24 months follow-up (n = 20)	*P*-value
MoCA, total (SD)	18.3 (5.5)	16.7 (6.0)	**0.038**	18.1 (4.4)	14.7 (6.8)	**0.008**	26.2 (2.2)	26.3 (2.7)	0.45
MDS-UPDRS, total (SD)	40.6 (22.9)	51.5 (27.6)	**0.014**	38.9 (23.2)	50.3 (17.7)	**0.037**	N/A	N/A	N/A
MDS-UPDRS-Part III (SD)	20.4 (13.1)	24.8 (15.5)	**0.049**	19.3 (13.0)	27.0 (12.9)	**0.004**	N/A	N/A	N/A
Hoehn & Yahr, score (SD)	1.5 (1.1)	2.0 (1.0)	0.069	1.4 (1.1)	1.9 (1.0)	0.14	N/A	N/A	N/A

Note: Bold indicates denotes statistical significance.
Abbreviations: DLB/MCI-LB, dementia with Lewy bodies/mild cognitive impairment with Lewy bodies; MoCA, Montreal Cognitive Assessment; SD, standard deviation; MDS-UPDRS, Movement Disorder Society-Sponsored Revision of the Unified Parkinson's Disease Rating Scale; N/A, not applicable.

FW change longitudinally between DLB/MCI-LB and control groups, we focused on ROIs with significant FW change identified in DLB/MCI-LB from baseline to 24 months. Many of the same ROIs showed significant effect of diagnosis on FW change after controlling for age, baseline FW, and imaging site (Table S2). These include middle and posterior cingula, inferior frontal, insula, parahippocampus, supramarginal, and Rolandic

TABLE 3 *Free-water changes over 12 to 24 months*

Significant ROIs at 12 and 24 months	Change in FW: 12 months–baseline (mean, SD)	FDR-corrected *P*-value	Change in FW: 24 months–baseline (mean, SD)	FDR-corrected *P*-value
Amygdala_L	0.011 (0.015)	**0.026**	0.025 (0.021)	**0.004**
Cingulum_Post_L	0.012 (0.015)	**0.022**	0.021 (0.012)	**<0.001**
Cingulum_Post_R	0.010 (0.013)	**0.026**	0.021 (0.018)	**0.004**
Entorhinal_Cortex_L	0.017 (0.027)	**0.050**	0.022 (0.027)	**0.023**
Parahippocampus_L	0.009 (0.012)	**0.022**	0.022 (0.022)	**0.011**
Insula_L	0.007 (0.009)	**0.022**	0.014 (0.015)	**0.011**
Insula_R	0.008 (0.010)	**0.022**	0.019 (0.017)	**0.006**
Fusiform_L	0.007 (0.010)	**0.026**	0.016 (0.017)	**0.012**
Retrosplenial_Cortex_R	0.007 (0.008)	**0.022**	0.021 (0.016)	**0.004**
Rolandic_Oper_L	0.013 (0.010)	**<0.001**	0.025 (0.026)	**0.011**
Rolandic_Oper_R	0.010 (0.013)	**0.022**	0.022 (0.019)	**0.005**
Supramarginal_R	0.005 (0.008)	**0.049**	0.012 (0.013)	**0.011**

Significant ROIs at 24 months only	Change in FW: 24 months–baseline (mean, SD)	FDR-corrected *P*-value
SN_Ant	0.024 (0.022)	**0.007**
SN_Post	0.029 (0.024)	**0.004**
Putamen_R	0.015 (0.017)	**0.022**
Pallidum_R	0.024 (0.032)	**0.041**
Amygdala_R	0.020 (0.024)	**0.022**
Cingulum_Mid_L	0.025 (0.01)	**<0.001**
Cingulum_Mid_R	0.014 (0.010)	**0.001**
Hippocampus_L	0.016 (0.018)	**0.019**
Hippocampus_R	0.016 (0.013)	**0.004**
Parahippocampus_R	0.018 (0.020)	**0.017**
Temp_Sup_R	0.018 (0.021)	**0.020**
Heschl_R	0.014 (0.016)	**0.020**
Frontal_Inf_Oper_L	0.016 (0.021)	**0.035**
Frontal_Inf_Orb_R	0.016 (0.020)	**0.026**
Fusiform_R	0.013 (0.016)	**0.024**
Precuneus_R	0.016 (0.016)	**0.011**
Retrosplenial_Cortex_L	0.022 (0.018)	**0.004**
Thalamus_R	0.011 (0.0112)	**0.012**

Note: There were two regions with significant FW change from baseline to 12 months (right lingual gyrus with mean FW change 0.010 ± 0.015 [pFDR = 0.040] and left pallidum with mean FW change 0.009 ± 0.012 [pFDR = 0.022]), but no corresponding significant FW change from baseline to 24 months. Bold indicates denotes statistical significance.

Abbreviations: ROI, region of interest; FW, free-water; SD, standard deviation; FDR, false discovery rate; L, left; Post, posterior; R, right; Oper, operculum; SN, substantia nigra; Ant, anterior; Mid, middle; Sup, superior; Inf, inferior; Orb, orbital.

operculum regions. Regions with significant FW change at 12 and/or 24 months in DLB/MCI-LB that did not exhibit significant group effect included the SN, amygdala, hippocampus, putamen, pallidum, fusiform, retrosplenial, superior temporal, thalamus, and precuneus (Tables 3 and S2).

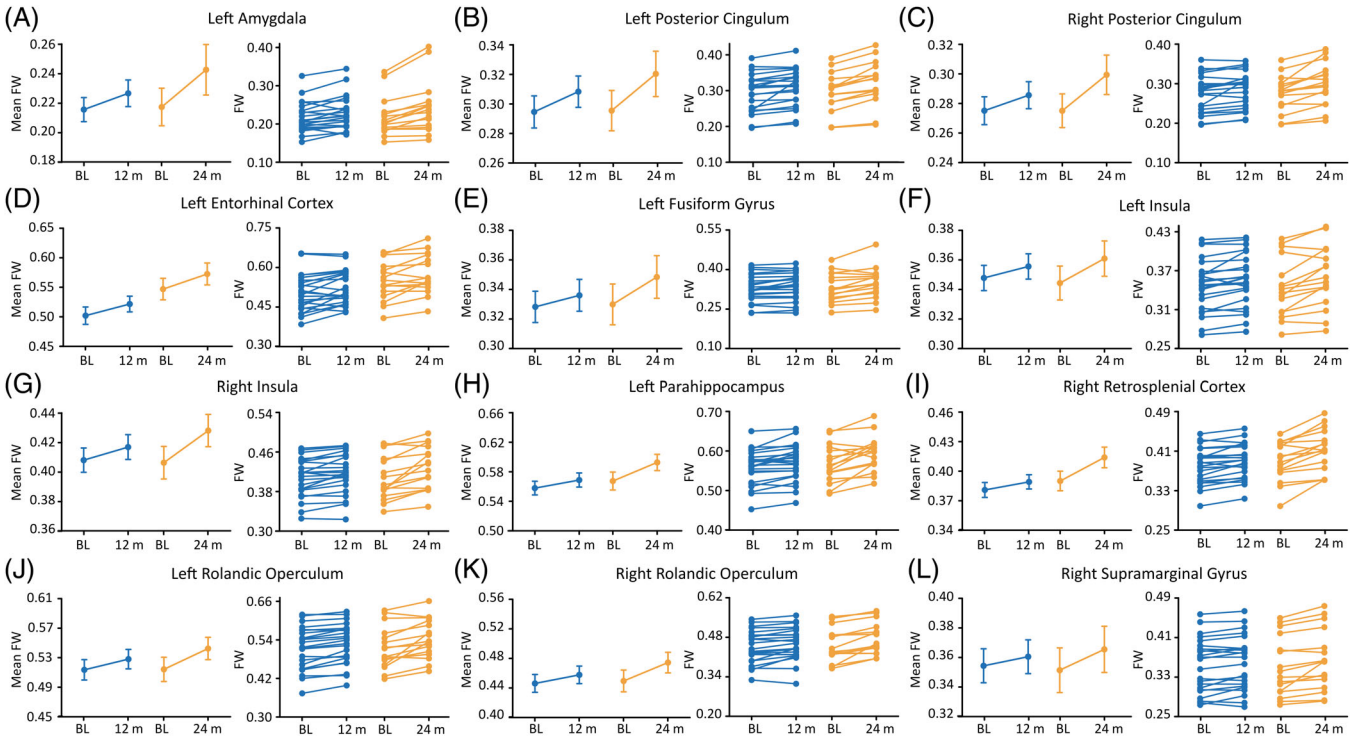

FIG. 1. (A–L): Regions of interest (ROIs) in dementia with Lewy bodies/mild cognitive impairment with Lewy bodies (DLB/MCI-LB) with significant increase in free-water (FW) from baseline to 12 (blue) and 24 months (orange). For each significant ROI, the corresponding plot on the left shows mean FW changes for each follow-up time point with standard error bars; and the corresponding plot on the right shows FW changes for each participant from baseline to 12 and 24 months. [Color figure can be viewed at wileyonlinelibrary.com]

Changes in Diffusion Measures Associated with DLB Clinical Progression

Exploratory forward linear regression analyses showed FW changes associated with clinical progression at 12 and 24 months in participants with DLB/MCI-LB. FW change was associated with a change in MDS-UPDRS total score from baseline to 12 months, with the final model including right insula (adjusted $R^2 = 22.2\%$, $P = 0.024$). Change in FW was also associated with a change in MDS-UPDRS total score from baseline to 24 months, with the final model including right amygdala, anterior SN, left fusiform, and left inferior frontal operculum (adjusted $R^2 = 93.5\%$, $P = 0.003$). FW change was associated with a change in MDS-UPDRS-Part III motor score from baseline to 24 months only, with the final model including the right amygdala (adjusted $R^2 = 0.679$, $P < 0.001$). FW change was associated with a change in MoCA score from baseline to 24 months only, with the final model including the left inferior frontal operculum (adjusted $R^2 = 42.6\%$, $P = 0.004$).

When evaluating potential associations between baseline FW and longitudinal clinical progression in DLB/MCI-LB, baseline FW was associated with a change in total MoCA score from baseline to 12 months only, with the final model including right posterior cingulum (adjusted $R^2 = 22.4\%$, $P = 0.026$). Baseline FW was associated with change in MDS-UPDRS-Part III motor from baseline to 24 months only, with the final model including left inferior frontal operculum, right Heschl gyrus, and posterior SN (adjusted $R^2 = 78.7\%$, $P = 0.017$).

Discussion

We found significant longitudinal FW increases in 12 ROIs at both 12 and 24 months' follow-up in individuals with DLB/MCI-LB. Additionally, we saw more ROIs with significant FW changes at 24 months, not detected at 12 months' follow-up. Many of these regions showed significant group effect at 24 months when comparing DLB/MCI-LB versus controls. We also found FW changes, and baseline FW, from selected ROIs in DLB/MCI-LB that were associated with clinical progression in MoCA and MDS-UPDRS scores. Together, these results provide evidence of longitudinal microstructural changes in DLB, seen as early as the 12 month follow-up. Furthermore, these diffusion changes are associated with cognitive and motor decline over 2 years.

Our results differ from the prior DTI-based longitudinal DLB study by Firbank et al.[21] where no MD or FA white matter changes were seen over 12 months. Notably, our study differs in study duration (24 vs. 12 months),

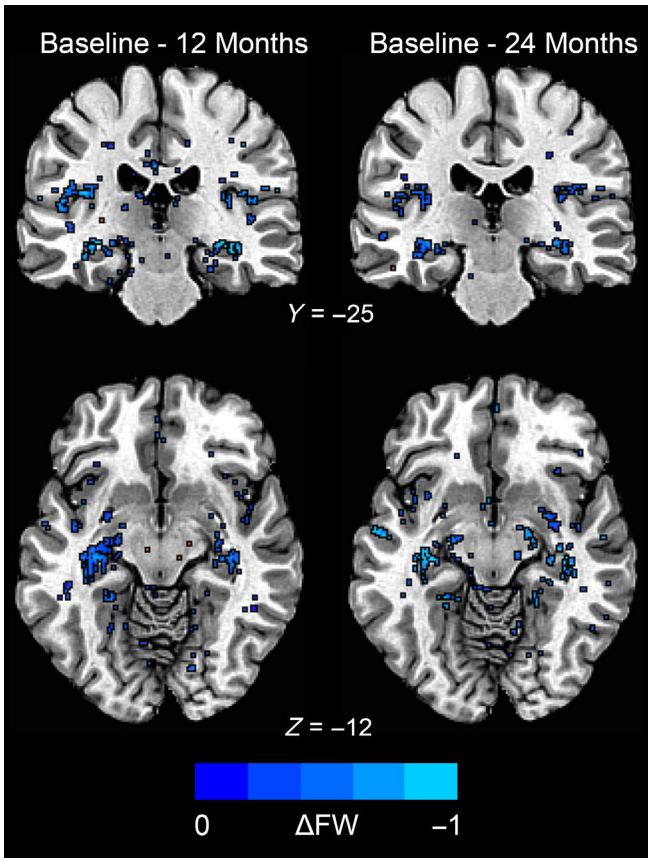

FIG. 2. T1-structural magnetic resonance imaging (MRI) (axial) showing larger network of regions of interest (ROIs) in dementia with Lewy bodies/mild cognitive impairment with Lewy bodies (DLB/MCI-LB) identified with significant free-water (FW) increases at 24 months (3D paired *t*-test for baseline to 24 months, right), compared to 12 months (3D paired *t*-test for baseline to 12 months, left). Overlay is displaying the mean difference in FW at $P < 0.001$ (uncorrected). The coordinate system is in Montreal Neurological Institute (MNI) space (with a left posterior inferior orientation). Consistent longitudinal FW increases at both time points were seen in amygdala, posterior cingulum, entorhinal cortex, parahippocampus, insula, fusiform, retrosplenial cortex, Rolandic operculum, and supramarginal gyrus regions. At 24 months, additional FW increases were seen in the pallidum, putamen, mid cingulum, hippocampus, inferior frontal, superior temporal, and thalamus regions. [Color figure can be viewed at wileyonlinelibrary.com]

approach (bi-tensor model vs. DTI), analysis (our custom dMRI pipelines[8,9,24] and MCALT use vs. tract-based spatial statistics), and primary outcome measures (FW vs. MD, FA). Considering that partial volume effects from extracellular FW can contaminate DTI analysis of microstructural changes, our FW approach may be more sensitive in detecting subtle microstructural changes involving gray matter regions.[39]

The consistent FW increases in DLB/MCI-LB cohorts involving the insula, amygdala, posterior cingulum, parahippocampal, entorhinal, supramarginal, fusiform, retrosplenial, and Rolandic operculum regions at both 12 and 24 months' follow-up suggest that microstructural changes may occur in these regions earlier in the disease course of DLB. Except for the amygdala, retrosplenial cortices, and fusiform, all the aforementioned regions were significant in both within-group (DLB/MCI-LB) and between-group models (DLB/MCI-LB vs. controls, baseline to 24 months). While the exact biological underpinnings of FW are still under investigation, FW changes in parahippocampal gyrus, amygdala, and cingulate gyrus align with prior DLB neuropathological studies showing increased α-synuclein burden in these limbic regions.[40] Similarly, early FW changes involving occipitotemporal and inferior temporal regions may correspond to underlying α-synuclein burden in neocortical regions of patients with DLB.[40]

From prior structural MRI studies, insular atrophy is consistently reported in prodromal DLB.[41] Cortical thinning in the right anterior insula may be a potential marker for early DLB[42] given its involvement in integrating autonomic, somatosensory, and cognitive information to guide behavior[43] (ie, relevant to cognitive slowing and attentional deficits in DLB). Significant FW increases in parahippocampal regions with earlier disease course is consistent with pathology studies showing disproportionate involvement of this region.[40] A prior study showed association of cortical thinning of parahippocampal and temporal pole regions with cognitive measures in DLB, but not AD.[44] Particularly relevant in DLB, early parahippocampal involvement may relate to its role in visuospatial processing.[45] Microstructural changes could reflect microglial activation/neuroinflammation or neurodegeneration seen in these regions.

Involvement of the visual association regions aligns with similar areas of the brain that were previously associated with microstructural changes in DLB.[13,23,46] The basal forebrain, inferior parietal (eg, supramarginal gyrus), and parahippocampal regions are highly interconnected and likely play a role in visual attention, and clinical symptoms of cognitive fluctuations and visual hallucinations.[11,16,46] Microstructural disruptions in the cingulum have been reported in prior studies,[23] and in our study we found early significant FW increases involving the posterior cingulate gyrus. We also detected longitudinal FW changes involving the precuneus at 24 months, though this significant within-group FW change was not seen when compared with the control group. This suggests the change in the precuneus for DLB may not exceed the variance and mean change of the control group. Characteristically in DLB on FDG-PET/SPECT scans, we expect relative sparing in posterior cingulate regions compared to cuneus/precuneus.[2] Additional study should investigate potential differential microstructural changes in the posterior cingulate versus cuneus/precuneus regions.

Early involvement of the entorhinal cortex aligns with the hypothesis that DLB preferentially affects brain regions with dense cholinergic inputs.[27,47] In a longitudinal structural MRI study following patients

with MCI-LB over a median of 1.3 years, significant atrophy in the nucleus basalis of Meynert was noted at baseline in MCI-LB versus controls, with more longitudinal atrophy including the entorhinal and parahippocampal gyri.[27] Atrophy progression occurred in regions with significant cholinergic innervation and aligned with clinical progression.[27] While we similarly found that FW changes in some ROIs correlated with clinical decline, we caution over-interpretating our exploratory regression analyses given the large numbers of significant ROIs and relatively small sample sizes.

Early FW changes involving the Rolandic operculum is a novel finding. Hypometabolism in the Rolandic operculum may play a role in sleep disturbance and RBD associated with DLB,[48] but more research is needed.

We identified more widespread cortical and subcortical involvement at 24-month follow-up in DLB/MCI-LB, involving the SN, pallidum, putamen, mid cingulum, hippocampus, inferior frontal, superior temporal, and thalamus. Changes in the mid cingulum and inferior frontal regions were significant in both within-group and between-group models. Additional studies should evaluate potential differential microstructural changes within *all* subregions of the cingulate.[23] Significant FW increases involving inferior frontal regions are consistent with prior fMRI and voxel-based morphometry studies in DLB. Structural changes in these regions may be associated with visuoperceptual impairments and visual hallucinations in DLB.[49]

Some of the regions with significant FW change at 24 months in the within-group (DLB/MCI-LB) but not between-group (DLB/MCI-LB vs. controls) approaches require further investigation. Basal ganglia and SN had significant FW changes in DLB/MCI-LB, but not when compared to controls. While basal ganglia atrophy is reported in DLB, the association between the degree of atrophy/neurodegeneration in the striatum and clinical parkinsonism is unclear.[50] Dopaminergic cell loss is often seen in the SN of patients with DLB, but this may be variable especially earlier in the disease course with α-synuclein distribution patterns (eg, brainstem-predominant, neocortical, limbic). The FW change we found in SN could be clinically relevant in DLB, as the posterior SN at baseline was associated with MDS-UPRS-III decline over 24 months, suggesting that FW changes prior to the baseline visit may predict long-term motor changes. Lack of hippocampal involvement (based on the between-group analysis) is not surprising, given that preservation of medial temporal regions and hippocampi are indicative biomarkers for DLB.[2] For some patients, hippocampal involvement reflects frequent AD co-pathology in DLB.[51]

This study has several limitations. Cohort sample sizes were modest, and MCI-LB was under-represented. However, our ability to detect significant diffusion changes with FDR correction even with a smaller cohort at 24 months argues for the robustness of the significant ROIs. Several regions (eg, SN, amygdala, retrosplenial cortex, fusiform) had significant longitudinal FW change in DLB/MCI-LB, but not when comparing DLB against controls, potentially due to age-related effects. Alternatively, the FW changes seen in these regions in DLB did not exceed the variance and mean change of controls. While controls were from a multisite database (ADNI), the same scanner was used for each control at all time points; additionally, we accounted for imaging site as a covariate in our ANCOVA model. We did not have fluid biomarkers or neuropathology to confirm Lewy body disease and evaluate co-pathologies. Future studies could investigate co-occurring cerebrovascular burden and concurrent tau/Aβ markers, and include a longitudinal AD cohort for comparison. We used a cognitive screening measure (MoCA) to assess global cognition. More detailed neuropsychological testing could further inform brain regions involved in DLB, though the optimal clinical outcome measures in DLB remain unclear.[52,53] Finally, our current study has limited generalizability due to inclusion of predominantly male, White, non-Hispanic individuals.

In summary, we applied a novel bi-tensor dMRI model to evaluate FW longitudinally in patients with DLB/MCI-LB over two time points. We identified a consistent set of regions associated with microstructural changes involving the insula, amygdala, posterior cingulum, parahippocampal, entorhinal, supramarginal, fusiform, retrosplenial, and Rolandic operculum regions over 12 and 24 months in DLB/MCI-LB. With longer follow-up, we found more widespread microstructural changes in regions implicated in visuospatial processing, motor, and cholinergic functions. Our results support FW imaging as a promising noninvasive and clinically relevant imaging marker that is sensitive to longitudinal disease progression in DLB. Replication in other datasets is needed before FW imaging is used as a biomarker for tracking DLB progression and potentially as a clinical trial endpoint for disease-modifying therapy. ■

Acknowledgments: We are grateful to our patients and their family members for participating in aging and dementia research.

Data Availability Statement

This study's data are available in the Parkinson's Disease Biomarker Program (https://pdbp.ninds.nih.gov) and ADNI database (http://adniloni.usc.edu).

References

1. Savica R, Boeve BF, Logroscino G. Epidemiology of alpha-synucleinopathies: from Parkinson disease to dementia with Lewy bodies. Handb Clin Neurol 2016;138:153–158.
2. McKeith IG, Boeve BF, Dickson DW, et al. Diagnosis and management of dementia with Lewy bodies: fourth consensus report of the DLB consortium. Neurology 2017;89(1):88–100.
3. McKeith IG, Ferman TJ, Thomas AJ, et al. Research criteria for the diagnosis of prodromal dementia with Lewy bodies. Neurology 2020;94(17):743–755.
4. Ferman TJ, Smith GE, Kantarci K, et al. Nonamnestic mild cognitive impairment progresses to dementia with Lewy bodies. Neurology 2013;81(23):2032–2038.
5. Kantarci K, Lesnick T, Ferman TJ, et al. Hippocampal volumes predict risk of dementia with Lewy bodies in mild cognitive impairment. Neurology 2016;87(22):2317–2323.
6. Kamagata K, Andica C, Kato A, et al. Diffusion magnetic resonance imaging-based biomarkers for neurodegenerative diseases. Int J Mol Sci 2021;22(10):5216.
7. Ofori E, DeKosky ST, Febo M, Colon-Perez L, Chakrabarty P, Duara R, et al. Free-water imaging of the hippocampus is a sensitive marker of Alzheimer's disease. Neuroimage Clin. 2019;24:101985.
8. Archer DB, Bricker JT, Chu WT, et al. Development and validation of the automated imaging differentiation in parkinsonism (AID-P): a multi-site machine learning study. Lancet Digit Health 2019;1(5):e222–e231.
9. Chu WT, Wang WE, Zaborszky L, et al. Association of cognitive impairment with free water in the nucleus basalis of Meynert and locus coeruleus to transentorhinal cortex tract. Neurology 2022;98(7):e700–e710.
10. Mori S, Zhang J. Principles of diffusion tensor imaging and its applications to basic neuroscience research. Neuron 2006;51(5):527–539.
11. Habich A, Wahlund LO, Westman E, Dierks T, Ferreira D. (Dis-) connected dots in dementia with Lewy bodies-a systematic review of connectivity studies. Mov Disord 2023;38(1):4–15.
12. Bozzali M, Falini A, Cercignani M, et al. Brain tissue damage in dementia with Lewy bodies: an in vivo diffusion tensor MRI study. Brain 2005;128(7):1595–1604.
13. Lee JE, Park HJ, Park B, Song SK, Sohn YH, Lee JD, Lee PH. A comparative analysis of cognitive profiles and white-matter alterations using voxel-based diffusion tensor imaging between patients with Parkinson's disease dementia and dementia with Lewy bodies. J Neurol Neurosurg Psychiatry 2010;81(3):320–326.
14. Watson R, Blamire AM, Colloby SJ, Wood JS, Barber R, He J, O'Brien JT. Characterizing dementia with Lewy bodies by means of diffusion tensor imaging. Neurology 2012;79(9):906–914.
15. Nedelska Z, Schwarz CG, Boeve BF, et al. White matter integrity in dementia with Lewy bodies: a voxel-based analysis of diffusion tensor imaging. Neurobiol Aging 2015;36(6):2010–2017.
16. Kantarci K, Avula R, Senjem ML, et al. Dementia with Lewy bodies and Alzheimer disease: neurodegenerative patterns characterized by DTI. Neurology 2010;74(22):1814–1821.
17. Ota M, Sato N, Ogawa M, Murata M, Kuno S, Kida J, Asada T. Degeneration of dementia with Lewy bodies measured by diffusion tensor imaging. NMR Biomed 2009;22(3):280–284.
18. Serra L, Cercignani M, Basile B, et al. White matter damage along the uncinate fasciculus contributes to cognitive decline in AD and DLB. Curr Alzheimer Res 2012;9(3):326–333.
19. Hattori T, Orimo S, Aoki S, et al. Cognitive status correlates with white matter alteration in Parkinson's disease. Hum Brain Mapp 2012;33(3):727–739.
20. Kiuchi K, Morikawa M, Taoka T, et al. White matter changes in dementia with Lewy bodies and Alzheimer's disease: a tractography-based study. J Psychiatr Res 2011;45(8):1095–1100.
21. Firbank MJ, Watson R, Mak E, et al. Longitudinal diffusion tensor imaging in dementia with Lewy bodies and Alzheimer's disease. Parkinsonism Relat Disord 2016;24:76–80.
22. Jensen JH, Helpern JA. MRI quantification of non-Gaussian water diffusion by kurtosis analysis. NMR Biomed 2010;23(7):698–710.
23. Delli Pizzi S, Franciotti R, Taylor JP, Esposito R, Tartaro A, Thomas A, et al. Structural connectivity is differently altered in dementia with Lewy body and Alzheimer's disease. Front Aging Neurosci 2015;7:208.
24. Ofori E, Pasternak O, Planetta PJ, et al. Longitudinal changes in free-water within the substantia nigra of Parkinson's disease. Brain 2015;138(8):2322–2331.
25. Mitchell T, Wilkes BJ, Archer DB, Chu WT, Coombes SA, Lai S, et al. Advanced diffusion imaging to track progression in Parkinson's disease, multiple system atrophy, and progressive supranuclear palsy. Neuroimage Clin 2022;34:103022.
26. Febo M, Perez PD, Ceballos-Diaz C, et al. Diffusion magnetic resonance imaging-derived free water detects neurodegenerative pattern induced by interferon-γ. Brain Struct Funct 2020;225(1):427–439.
27. Kantarci K, Nedelska Z, Chen Q, et al. Longitudinal atrophy in prodromal dementia with Lewy bodies points to cholinergic degeneration. Brain Commun 2022;4(2):fcac013.
28. Ferman TJ, Smith GE, Boeve BF, et al. DLB fluctuations: specific features that reliably differentiate DLB from AD and normal aging. Neurology 2004;62(2):181–187.
29. American Academy of Sleep Medicine. International classification of sleep disorders. Diagnostic and Coding Manual; Westchester, IL: American Academy of Sleep Medicine; 2005:148–152.
30. Goetz CG, Tilley BC, Shaftman SR, Stebbins GT, Fahn S, Martinez-Martin P, et al. Movement Disorder Society-sponsored revision of the Unified Parkinson's Disease Rating Scale (MDS-UPDRS): scale presentation and clinimetric testing results. Mov Disord 2008;15(23):2129–2170.
31. Pasternak O, Sochen N, Gur Y, Intrator N, Assaf Y. Free water elimination and mapping from diffusion MRI. Magn Reson Med 2009;62(3):717–730.
32. Leemans A, Jones DK. The B-matrix must be rotated when correcting for subject motion in DTI data. Magn Reson Med 2009;61(6):1336–1349.
33. FSL. [December 15, 2023]; Available from: https://fsl.fmrib.ox.ac.uk/fsl/fslwiki/.
34. Advanced Normalization Tools. [December 15, 2023]; Available from: http://stnava.github.io/ANTs/.
35. Schwarz CG, Gunter JL, Ward CP, et al. The Mayo Clinic Adult Lifespan Template (MCALT): better quantification across the lifespan. Alzheimers Dement 2017;13:93–94.
36. Chen Q, Boeve BF, Forghanian-Arani A, et al. MRI quantitative susceptibility mapping of the substantia nigra as an early biomarker for Lewy body disease. J Neuroimaging 2021;31(5):1020–1027.
37. Chen Q, Przybelski SA, Senjem ML, et al. Longitudinal tau positron emission tomography in dementia with Lewy bodies. Mov Disord 2022;37(6):1256–1264.
38. Benjamini Y, Hochberg Y. Controlling the false discovery rate: a practical and powerful approach to multiple testing. J R Stat Soc B Methodol 1995;57(1):289–300.
39. Ofori E, Krismer F, Burciu RG, et al. Free water improves detection of changes in the substantia nigra in parkinsonism: a multisite study. Mov Disord 2017;32(10):1457–1464.
40. Ferman TJ, Aoki N, Crook JE, et al. The limbic and neocortical contribution of alpha-synuclein, tau, and amyloid beta to disease duration in dementia with Lewy bodies. Alzheimers Dement 2018;14(3):330–339.
41. Roquet D, Noblet V, Anthony P, et al. Insular atrophy at the prodromal stage of dementia with Lewy bodies: a VBM DARTEL study. Sci Rep 2017;7(1):9437.
42. Blanc F, Colloby SJ, Philippi N, de Petigny X, Jung B, Demuynck C, et al. Cortical thickness in dementia with Lewy bodies and Alzheimer's disease: a comparison of prodromal and dementia stages. PloS One 2015;10(6):e0127396.
43. Christopher L, Koshimori Y, Lang AE, Criaud M, Strafella AP. Uncovering the role of the insula in non-motor symptoms of Parkinson's disease. Brain 2014;137(Pt 8):2143–2154.

44. Elder GJ, Mactier K, Colloby SJ, Watson R, Blamire AM, O'Brien JT, Taylor JP. The influence of hippocampal atrophy on the cognitive phenotype of dementia with Lewy bodies. Int J Geriatr Psychiatry 2017;32(11):1182–1189.

45. Aminoff EM, Kveraga K, Bar M. The role of the parahippocampal cortex in cognition. Trends Cogn Sci 2013;17(8):379–390.

46. Zorzi G, Thiebaut de Schotten M, Manara R, Busse C, Corbetta M, Cagnin A. White matter abnormalities of right hemisphere attention networks contribute to visual hallucinations in dementia with Lewy bodies. Cortex 2021;139:86–98.

47. Schumacher J, Ray NJ, Hamilton CA, et al. Cholinergic white matter pathways in dementia with Lewy bodies and Alzheimer's disease. Brain 2022;145(5):1773–1784.

48. Iaccarino L, Marelli S, Iannaccone S, Magnani G, Ferini-Strambi L, Perani D. Severe brain metabolic decreases associated with REM sleep behavior disorder in dementia with Lewy bodies. J Alzheimers Dis 2016;52(3):989–997.

49. Mak E, Su L, Williams GB, O'Brien JT. Neuroimaging characteristics of dementia with Lewy bodies. Alzheimers Res Ther 2014;6(2):18.

50. Cousins DA, Burton EJ, Burn D, Gholkar A, McKeith IG, O'Brien JT. Atrophy of the putamen in dementia with Lewy bodies but not Alzheimer's disease: an MRI study. Neurology 2003;61(9):1191–1195.

51. Kantarci K, Lowe VJ, Chen Q, et al. Beta-amyloid PET and neuropathology in dementia with Lewy bodies. Neurology 2020;94(3):e282–e291.

52. Patel B, Irwin DJ, Kaufer D, Boeve BF, Taylor A, Armstrong MJ. Outcome measures for dementia with Lewy body clinical trials: a review. Alzheimer Dis Assoc Disord 2022;36(1):64–72.

53. Rodriguez-Porcel F, Wyman-Chick KA, Abdelnour Ruiz C, et al. Clinical outcome measures in dementia with Lewy bodies trials: critique and recommendations. Transl Neurodegener 2022;11(1):24.

Supporting Data

Additional Supporting Information may be found in the online version of this article at the publisher's web-site.

SGML and CITI Use Only
DO NOT PRINT

Author Roles

(1) Research Project: A. Conception, B. Organization, C. Execution; (2) Statistical Analysis: A. Design, B. Execution, C. Review and Critique; (3) Manuscript Preparation: A. Writing of the First Draft, B. Review and Critique.

S.Y.C.: 1A, 1B, 1C, 2A, 2B, 2C, 3A, 3B.
R.C.: 1A, 1B, 2A, 2B, 2C, 3B.
W.W.: 1A, 1B, 2A, 2B, 2C, 3B.
M.J.A.: 2C, 3B.
B.F.B: 3B.
R.S.: 3B.
V.R.: 3B.
J.A.F.: 3B.
N.G.-R.: 3B.
T.J.F.: 3B.
K.K.: 2C, 3B.
D.E.V.: 1A, 1B, 2A, 2C, 3B.

Financial Disclosures of All Authors (for the Preceding 12 Months)

S.Y.C. receives research support from NIH (K23 AG073525-01A1), Harry T. Mangurian Jr. Foundation, and Smallwood Foundation. R.C. has no relevant disclosures. W.W. has no relevant disclosures. M.J.A. receives research support from the National Institutes of Health (NIH) (R01AG068128, P30AG047266, R01NS121099, R44AG062072), and as the local PI of a Lewy Body Dementia Association Research Center of Excellence. She serves on the DSMBs for the Alzheimer's Therapeutic Research Institute/Alzheimer's Clinical Trial Consortium and the Alzheimer's Disease Cooperative Study. She has provided educational content for Medscape. B.F.B. receives honorarium for scientific advisory board (SAB) activities for the Tau Consortium, institutional research grant support from the Lewy Body Dementia Association, American Brain Foundation, Alector, Biogen, Transposon, and GE Healthcare. R.S. receives support from the National Institute on Aging, the National Institute of Neurological Disorders and Stroke, the Parkinson's Disease Foundation, and Acadia Pharmaceuticals. V. Ramanan receives research support from NIH. J.A.F. receives research support from NIH. N.G.-R. receives research support as the local PI of a Lewy Body Dementia Association Research Center of Excellence and from NIH. T.J.F. receives research support from NIH, the Mayo Clinic Dorothy and Harry T. Mangurian Jr. Lewy Body Dementia Program, and Ted Turner and Family LBD Functional Genomics Program. K.K. receives research support from NIH, Avid Radiopharmaceuticals, Eli Lilly, and consults for Biogen. D.E.V. receives research support from NIH.